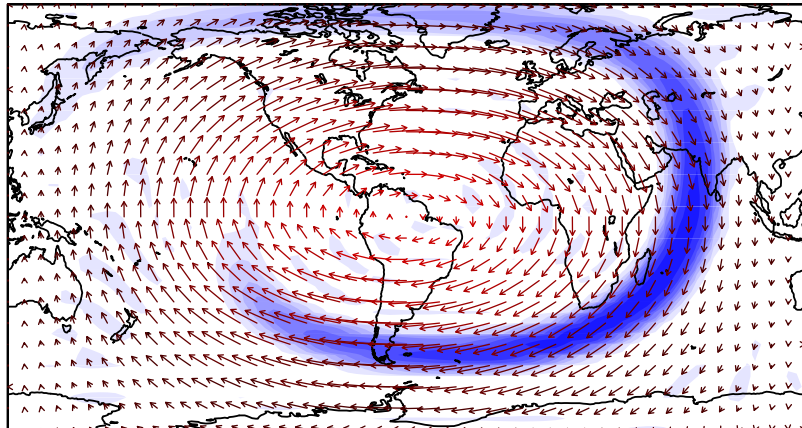


Mark Schlutow

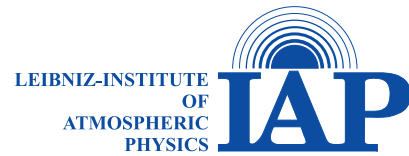
A Positive Definite Scheme for Mass Conserving Spectral Tracer Transport in Global Climate Models



Universität
Rostock



Traditio et Innovatio



A Positive Definite Scheme for Mass Conserving Spectral Tracer Transport in Global Climate Models

Diploma Thesis

submitted at the Institute of Physics

University of Rostock

Mark Schlutow

February 7, 2012

1st Reviewer: Erich Becker, Leibniz-Institute of Atmospheric Physics e.V. at the
University of Rostock, Kühlungsborn

2nd Reviewer: Heiner Körnich, Department of Meteorology, Stockholm University

Abstract

We present a new three-dimensional tracer transport scheme for spectral atmospheric general circulation models including advection and diffusion. In order to achieve strong stability and high consistency, it is argued for a spectral transport scheme in a spectral circulation model. A new function of representation that assures positive definite tracer mass mixing ratios and a new effective mass correction at low computational cost are proposed. The mass correction guarantees global tracer mass conservation. It is designed in a manner that it is minimally invasive by introducing a mighty parameter adjustable to the problem. The scheme is benchmarked with two deformational flow test cases challenging the horizontal and vertical numerical advection with respect to the conservation laws. For this reason the concept of the entropy of mixing is adopted to the tracer transport. This makes it possible to evaluate quantitatively the impact on the results by artificial diffusion and other numerical uncertainties. In particular, it is found that the control parameter of the proposed mass correction governs the balance between the conservation of total mass and total entropy of mixing.

Contents

Abstract	v
1 Introduction	1
1.1 Motivation	1
1.2 Aim	3
1.3 Framework	3
2 Theory of Tracer Transport	5
2.1 From Mass Conservation to the Transport Equation	5
2.2 From Fundamental Thermodynamic Laws to the Entropy of Mixing .	7
2.2.1 Deriving the Entropy of Mixing	8
2.2.2 Verifying the Entropy of Mixing	10
2.2.3 Negentropy of Mixing and Further Implications	12
3 Numerical Treatment of the Transport Equation	15
3.1 The Kühlungsborn Mechanistic General Circulation Model	15
3.2 On the Issue of Aliasing	15
3.3 A Function of Representation for Positive Definite Mixing Ratios . .	18
3.4 A Mass Correction for General Circulation Models	20
4 Validating the scheme	25
4.1 Initial Condition	26
4.2 Non-Divergent Flow	26
4.3 Purely Divergent Flow	27
4.4 Assessing the Total Entropy of Mixing	28
4.5 Analysis and Results of the Benchmarks	29

Contents

5 Conclusion	37
5.1 Summary	37
5.2 Implications and Future Tasks	38
Bibliography	41

1 Introduction

1.1 Motivation

Transport plays a crucial role in understanding the leading processes and dynamics in modern atmospheric science. The evolution of trace gases such as carbon dioxide (CO_2) or ozone as well as water vapor and other species has a significant influence on the entire climate and therefore on human life.

For example, the water vapor cycle has an essential impact on the greenhouse effect and hence on global warming as it controls the global radiation budget significantly. On the one hand, clouds are reflective for incoming solar radiation, especially in the visible spectrum, which cools the earth's surface. On the other hand, they absorb outgoing long-wave radiation heating the surface. The result is an uncertain balance that is hard to mimic in circulation models. Only the physically correct interpretation of the transport processes makes it possible to predict certain results.

Furthermore, stratospheric water vapor is of high interest in current research as it is an effective long-wave cooling agent. The challenging aspect is that transport in the troposphere regarding clouds takes place on short time scales, mainly days, whereas water vapor takes years to enter particular regions in the stratosphere.

In addition to water, CO_2 represents one anthropogenic part in the intensification of the greenhouse effect. Its man-made sources at the surface affect this complicated radiation balance. While CO_2 is rapidly mixed in the troposphere, it takes years again to be transported into the extratropical stratosphere by the Brewer-Dobson circulation.

Ozone depletion provides another example. As the chemical sources and sinks of ozone vary substantially between tropical and polar latitudes in the stratosphere, the transport between these regions plays an important role.

The examples above demonstrate the need of precise transport algorithms in global climate models obeying the physical laws as good as possible. These laws

1 Introduction

are energy, momentum, angular momentum, and of course mass conservation governed by the primitive equations. But actually, we must also take account of the entropy budget which is as important as the internal energy budget since both together correspond to the second and first law of thermodynamics. The achievement of energy conservation in a global climate model causes a violation of the entropy budget because of numerical errors. Therefore, the estimation of the global entropy budget could provide a crucial measure for the obedience of the physical laws.

Jöckel (2001), Rood (1987), Nair and Lauritzen (2010), and Williamson and Rasch (1994) demand the following requirements for numerical transport schemes: Mass conservation, monotonicity preservation or rather shape preservation, sign-preservation, and prevention of artificial diffusivity. Besides mass all the other properties are more of a technical or mathematical nature. This work proposes the use of the total entropy as a diagnostic variable for evaluating transport schemes since the entropy is more physically based. And we presume that consistency of a transport scheme has to be measured by answering the question: Is the result physically maintainable? Especially, for long-term simulations covering several model years the “physical consistency” of the transport algorithm is crucial. Pauluis and Held (2002) give an extended overview about the entropy budget in the atmosphere but without any particular numerical implications. In contrast, Minoshima et al. (2011) treated the entropy solely mathematically without referencing to its physical equivalent. This work suggests that entropy and mass conservation are equally important for the “physical consistency” of transport schemes.

In order to specify the transport processes we will consider transport only of tracer. Tracer are particles or fluid properties following the flow trajectories. As we assume that air is an ideal gas, any tracer particle must have the same properties as the air. In contrast, heavier particles have higher inertial mass so that accelerating forces act differently on them, which results in different trajectories. Tracer are used to make transport mechanisms observable. In the atmosphere CO₂ or sulfur hexafluoride (SF₆) (Engel et al., 2009) can be used as tracer, because they are hardly chemically reactive and their sources are well known. For short-term observations dye tracer are appropriate. But temperature can also be a tracer in a suitable experiment. Even abstract dimensions like “idealized age tracer” for the computation of the “mean

age of air” (Thiele and Sarmiento, 1990).

1.2 Aim

The aim of this work is to develop a numerical scheme for tracer transport in spectral general circulation models. We are especially interested in long-term simulations. It is planned in advance to simulate the “mean age of air” as one of the first applications of this scheme in a more realistic climate model. Therefore, the conservation laws are supposed to play an essential role as only purely physical transport can represent a realistic behavior with high “physical consistency” of tracer even after several model years. Since every numerical scheme is associated with numerical errors, compromises must be made that fit best to the constraints of the issue. Here, the primary demands on the scheme are that it provides positive definite results, i.e. sign-preservation, and that the total mass of a tracer is conserved. Furthermore, the transport scheme is supposed to be computationally fast and at low cost since global climate models must handle diverse species that even interact with the flow at the same time. As this work is additionally meant as a feasibility study, benchmark test cases and diagnostic methods are needed in order to evaluate the proposed scheme with respect to its constraints.

1.3 Framework

In section 2 we will derive the transport equation and the entropy of mixing from the fundamental laws of thermodynamics. We will see that it is possible to obtain two different versions of the transport equation: One from mass conservation and the other from entropy observation. Furthermore, the relation between the entropy of mixing and properties demanded for numerical transport schemes, e.g. monotonicity preservation, will be analyzed.

The model used for implementing the scheme and its properties is introduced in section 3. We will give a brief review of the aliasing effect which is associated with the spectral method.

These considerations will motivate the need of a new function of representation (section 3.3) that ensures sign-preserving results. This function is the new prognostic

1 Introduction

variable in the transport equation.

Section 3.4 will introduce a mass correction that has become necessary since the numerics with the new function of representation are no longer mass conserving.

Two different challenging benchmark deformational flow test cases for the horizontal and vertical transport will be applied in section 4 in order to validate the proposed scheme. The results will be analyzed with special attention to mass and entropy conservation evaluating the stability and “physical consistency”.

The last section gives a summary and shows some perspectives for further applications of the concept of the entropy of mixing.

2 Theory of Tracer Transport

2.1 From Mass Conservation to the Transport Equation

In the following section we develop the theory governing the tracer transport in a model. And furthermore, we discuss qualities, in particular the entropy of mixing, making it possible to evaluate a numerical transport scheme regarding whether the numerical errors behave physical or not. In general, a tracer is an arbitrary fluid property used to track transport processes in the flow. It is possible to use special chemical species, e.g. trace gases, but also potential temperature or artificial dye tracer are appropriate.

For the purpose of characterizing tracer a few terms are defined. We distinguish between active, passive, conservative, and reactive tracer. Active tracer alter flow properties such as density or viscosity whereas passive tracer do not interact with the flow. Conservative tracer are only advected so that the mixing ratio of the tracer remains constant in time in a fluid parcel following the flow. In addition to advection, reactive tracer are diffusive and have sources or sinks so that the mixing ratio in a parcel varies in time.

In this work we treat only passive, diffusive tracer whereas neither sources nor sinks are involved, i.e. the global mass is conserved. This concept is governed by the advection-diffusion equation, hereafter referred as the transport equation.

In order to illustrate the theory behind tracer transport mechanisms we use the picture of fluid parcels that consist of fluid particles namely air particles and tracer particles. Obviously, a single air particle does not exist as air is a composition of several gases. But since we describe air as an ideal gas, the image of an air particle is reasonable. Tracer particles must have the same thermodynamic properties like mass and temperature as air particles. However, they are made distinguishable from each other by a marker. This marker could be any color. We suggest to paint air particles white and tracer particles blue.

2 Theory of Tracer Transport

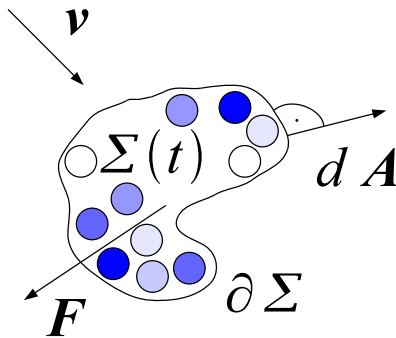


Figure 2.1: Sketch of a fluid control volume Σ with the boundary $\partial\Sigma$ attached to a wind field \mathbf{v} . The control volume contains fluid parcels (circles) which contain tracer and air particles. Their mass mixing ratios are indicated by different tones of blue.

We consider an arbitrary finite control volume $\Sigma(t)$ exposed to the fluid flow. This volume contains a definite number of fluid parcels which are associated with the thermodynamic properties. In the absence of sources and sinks, mass conservation states that, no matter how this parcel is deformed or displaced, its total mass (number of fluid parcels) must not vary:

$$d_t \int_{\Sigma(t)} dm = d_t \int_{\Sigma(t)} dV \rho(t) = 0 \quad (2.1)$$

In (2.1) the differential mass dm is substituted by the differential volume dV and the total density ρ . Applying the Leibniz integral rule results in the Reynolds' transport theorem.

$$d_t \int_{\Sigma(t)} dV \rho(t) = \int_{\Sigma(t)} dV \partial_t \rho(t) + \oint_{\partial\Sigma(t)} d\mathbf{A} \cdot \mathbf{v}(t) \rho(t) \quad (2.2)$$

Here, $\mathbf{v} = d_t \mathbf{r}$ is the flow velocity and $d\mathbf{A}$ a vector perpendicular to the surface of Σ with the differential surface area in length. Employing Gauss' theorem on the right hand side of (2.2), using condition (2.1), and considering the limiting case of an infinitesimally small control volume (i.e. the control volume approaches to the size of a fluid parcel) we obtain the continuity equation.

$$\partial_t \rho + \nabla \cdot (\rho \mathbf{v}) = 0 \quad (2.3)$$

2.2 From Fundamental Thermodynamic Laws to the Entropy of Mixing

We now assume that the fluid consists of two species: air (A) and a tracer (T), i.e.

$$\rho = \rho_A + \rho_T . \quad (2.4)$$

In order to express both species in terms of the total density the mass mixing ratio c is introduced with

$$\rho_T = c\rho \quad \text{and} \quad \rho_A = (1 - c)\rho . \quad (2.5)$$

Similar to (2.3) it is possible to derive a continuity equation for the tracer. But with the difference that some net transport exists through the boundaries of the control volume due to diffusion in such a manner that tracer material escaping the control volume needs to be compensated by an air current into it. This process is accomplished by the tracer diffusion flux $\mathbf{F} = \rho K \nabla c$ and by a corresponding air diffusion flux balancing it. Here, the diffusion coefficient K is composed of eddy and molecular diffusion.

$$\partial_t(c\rho) + \nabla \cdot (c\rho\mathbf{v}) = \nabla \cdot (\rho K \nabla c) \quad (2.6)$$

Combining equation (2.3) and (2.6) results in the transport equation for the tracer.

$$\partial_t c + \mathbf{v} \cdot \nabla c = \rho^{-1} \nabla \cdot (\rho K \nabla c) \quad (2.7)$$

In addition to the separation of air and tracer in the fluid parcel it is necessary to pay attention to the primitive equations (PE) governing the dynamic processes in the atmosphere. There is no difference between tracer and air in the PE, only the total density occurs as a diagnostic variable. For the purpose of simplicity it is approximated that the tracer does not contribute to the total air mass significantly. Thus, we assume that the total density is equal to the air density approximately and further the mass mixing ratio is small.

2.2 From Fundamental Thermodynamic Laws to the Entropy of Mixing

Numerical schemes solving equation (2.7) should satisfy several constraints: In addition to the global mass conservation, schemes should fulfill qualities like sign- and

2 Theory of Tracer Transport

monotonicity-preservation, diminishment of the total variation (Durrant, 2010), prevention of aliasing etc.. These qualities are more of a mathematical nature as their physical relevance is not obvious. But maybe, they actually mimic the behavior of the entropy which is probably not a very intuitive dimension but in return a very physical. Another argument for the importance of the entropy lies within the fundamental laws of thermodynamics. When considering the internal energy of a system, it is crucial to take the entropy into account regarding the first and second law of thermodynamics. In comparison to the internal energy, in fluid motions the mass is the conserved quality due to transport, and consequently the additional quality is the so called entropy of mixing. The entropy of mixing is mathematically very close to Shannon's information entropy (see Minoshima et al. (2011)), but as mentioned above we are more interested in its physical equivalence.

2.2.1 Deriving the Entropy of Mixing

In the following, a derivation of the entropy produced by mixing a tracer into the air is presented. The mixing process is meant to be driven by the transport equation (2.7) and further as the tracer is passive, the entropy is supposed to depend only on the mixing ratio of the tracer since it is the prognostic variable. In order to derive the total entropy due to mixing, the fluid parcels are divided into mass fractions $\Delta m = \Delta m_A + \Delta m_T$ consisting of the two gases, air and the tracer. First of all, we compute the entropy s for each Δm by combining the first and second law of thermodynamics:

$$du = T ds + dw \tag{2.8}$$

And finally, all s will be summed up to obtain the global budget of the entropy of mixing, hereafter referred as the total entropy of mixing S . Mixing changes neither the internal energy u nor the temperature T as long as the tracer is passive. So that no kind of heat, e.g. latent heat or heat of mixing, is produced irreversibly and hence no change of the entropy occurs in equation (2.8). Therefore, a reversible, equivalent thermodynamic process is necessary. We propose to separate air and tracer particles in each fluid parcel. This process is described by the compression of each constituent into its own available volume as shown in figure 2.2. Thus, every fluid parcel is no longer in the state of local equilibrium corresponding to the

2.2 From Fundamental Thermodynamic Laws to the Entropy of Mixing

maximum entropy. The separation results in a state of minimal entropy instead. The reverse process mimics the production of entropy due to mixing. This can be expressed by the volume-pressure work $dw = p_A dv + p_T dv$. Using the equation of

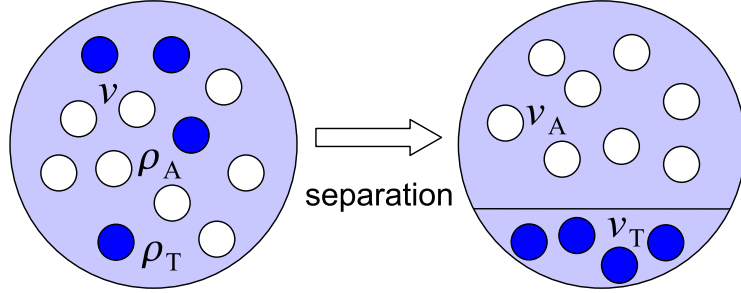


Figure 2.2: Sketch of separating air (white dots) and tracer (blue dots) particles by compressing each into its own available volume in a fluid parcel (circle).

state for ideal gases for the tracer as well as for air

$$p_j v = \Delta m_j R T \quad (2.9)$$

with $j = A, T$ combined with (2.8) provides the entropy of mixing in a fluid parcel by integration from the state of demixing to the current state.

$$s = R \left(\Delta m_A \ln \frac{v}{v_A} + \Delta m_T \ln \frac{v}{v_T} \right) \quad (2.10)$$

Note that a similar approach can be found in literature, e.g. Nolting (2005). The volumes v_A and v_T can be derived by assuming that the pressure in both volumes must be equal as well as using $v = v_A + v_T$. Furthermore, v_A and v_T can be represented by the densities and finally by the mass mixing ratio $\rho_T = c\rho$ (see (2.5)). If we presume that $c \ll 1$, then we can set $\rho_A \approx \rho$. With this assumption the first summand on the right hand side of equation (2.10) vanishes as the work done on the air particles is negligible. By applying the infinitesimal limit $\Delta m_T \rightarrow dm_T = dV \rho c$ it is possible to substitute the summation over all Δm by an integral over the entire atmosphere in order to derive the total entropy of mixing.

$$S = -R \int dV \rho c \ln c \quad (2.11)$$

2 Theory of Tracer Transport

Note that equation (2.11) describes the change in entropy from a state of total demixing, which we assume to refer to the minimum entropy, to the current distribution represented by c . The maximum total entropy of mixing should be obtained by reaching the state of equal distribution.

2.2.2 Verifying the Entropy of Mixing

Possibly, the latest approximations are physically unreasonable. In order to prove that equation (2.11) indeed refers to the correct entropy of the system, one can compute the change of the total entropy of mixing in time during the advection and diffusion of the tracer by applying the time derivative on S and taking advantage of the continuity equation of both the air (2.3) and the tracer (2.6).

By applying the time derivative on (2.11) and taking advantage of the product rule we obtain:

$$d_t S = -R \int dV \partial_t (\rho c \ln c) = -R \int dV (\partial_t (c\rho) \ln c + \rho \partial_t c) \quad (2.12)$$

We further insert the continuity equations (2.6) and (2.7)

$$\begin{aligned} d_t S = -R \int dV & ((\nabla \cdot (\rho K \nabla c) - \nabla \cdot (c\rho \mathbf{v})) \ln c \\ & + \rho (\rho^{-1} \nabla \cdot (\rho K \nabla c) - \mathbf{v} \cdot \nabla c)) \end{aligned} \quad (2.13)$$

And by the use of the product rule for a scalar Φ multiplied by a vector \mathbf{U} ,

$$\nabla \cdot (\Phi \mathbf{U}) = \mathbf{U} \cdot \nabla \Phi + \Phi \nabla \cdot \mathbf{U} ,$$

2.2 From Fundamental Thermodynamic Laws to the Entropy of Mixing

we find:

$$\begin{aligned}
 d_t S = -R \int dV & (\nabla \cdot (\rho K \ln c \nabla c) \\
 & - \rho K c^{-1} (\nabla c)^2 \\
 & + \nabla \cdot (c \rho \ln c \mathbf{v}) \\
 & + \rho \mathbf{v} \cdot \nabla c \\
 & + \nabla \cdot (\rho K \nabla c) \\
 & - \rho \mathbf{v} \cdot \nabla c)
 \end{aligned} \tag{2.14}$$

Finally the Gauss' theorem is applied and it is presumed that all fluxes through the boundaries of the atmosphere must vanish.

$$d_t S = R \int dV \rho K c^{-1} (\nabla c)^2 \tag{2.15}$$

Pauluis and Held (2002) describe the irreversible entropy production due to diffusion of water vapor. By expressing (2.15) in terms of the diffusion flux we gain the same result.

$$d_t S = R \int dV \mathbf{F} \nabla \ln c \tag{2.16}$$

To put it in a nutshell, we verified that (2.11) is a reasonable expression for the total entropy of mixing. Furthermore, (2.15) has several qualities that will be discussed briefly. First, the tendency of the total entropy of mixing depends on K , but not on \mathbf{v} . Only diffusion can change the total entropy of mixing, advection is a reversible process, as it should be. Second, only if K , ρ and c are positive, which is the natural, physical case, then the total entropy of mixing is monotonically increasing as expected. Note, the monotonicity does not depend on the gradient of c as it is squared and hence the affected term is positive anyway. If c approaches zero, then equation (2.15) can only converge if the term $(\nabla c)^2$ is also vanishing. Additionally, previous considerations give strong arguments in order to require the positivity of mixing ratios of tracer in numerical models. Third, the tendency becomes zero and hence the total entropy of mixing reaches an extremum if ∇c is vanishing which

2 Theory of Tracer Transport

occurs in case of c approaching to its global mean value \bar{c} defined by:

$$\bar{c} = \frac{\int dV \rho c}{\int dV \rho} \quad (2.17)$$

It is obvious that this extremum is a global maximum as the total entropy of mixing is monotonically increasing and further the vanishing gradient stops the mass transfer due to diffusion. Inserting $c = \bar{c}$ in equation (2.11) and taking advantage of the definition (2.17) yield the maximum entropy:

$$S_{max} = -R \int dV \rho c \ln \bar{c} \quad (2.18)$$

2.2.3 Negentropy of Mixing and Further Implications

A more convenient quantity than the entropy is the so called negentropy or rather negative free entropy:

$$J = S_{max} - S = R \int dV \rho c \ln \frac{c}{\bar{c}} \quad (2.19)$$

It denotes the difference between the actual, current entropy and the maximum entropy. It is positive definite and decreases in time during irreversible mixing. While reaching the equilibrium, the total negentropy of mixing converges to zero. Equation (2.19) will be applied for numerical analysis in section 4.5.

In comparison to section 2.1, where we derived the transport equation from mass conservation, it is also possible to obtain an equivalent transport equation from entropy conservation. Since the entropy of mixing per unit mass is given by $s = -Rc \ln c$, its material time rate of change is:

$$\partial_t s + \mathbf{v} \cdot \nabla s = \rho^{-1} \nabla \cdot (\rho K \nabla s) + RK \frac{(\nabla c)^2}{c} \quad (2.20)$$

Here, c is a functional depending on s . As this functional is not bijective, it is not possible to compute c or rather the production term in (2.20) definitely and hence this version of the transport equation is a little bit inconvenient. But nevertheless, it must be acknowledged that (2.20) and (2.7) are equivalent transport

2.2 From Fundamental Thermodynamic Laws to the Entropy of Mixing

equations. Solving these equations with a conservative numerical scheme one can choose between mass or entropy of mixing conservation with respect to advection and diffusion of c or s , respectively.

How is the monotonicity associated with the entropy of mixing? A method is monotonicity preserving if it conserves monotone-increasing or monotone-decreasing initial data (Durrant, 2010). This means, in particular, that no new local extrema are generated which is similar to shape and sign-preservation. Considering the entropy of mixing as a measure of disorder: If monotonicity preservation is violated because new local extrema occur during the time evolution, then the entropy of the system is reduced. This seems rational since every new local extremum is an indication of a higher state of order, and hence less disorder, which is equivalent to a decreasing entropy.

Another commonly used diagnostic measure is the total variance σ^2 . It can be used as an additional conserved quantity in advection schemes (Prather, 1986). Here, it is defined as:

$$\sigma^2 = \frac{\int dV \rho c'^2}{\int dV \rho} \quad (2.21)$$

The term c' is obtained by the decomposition of c in $c = \bar{c} + c'$. The total variance is conserved by advection and reduced due to diffusion. All in all, it seems to display the same behavior as the total negentropy of mixing. In fact, negentropy and variance are related closely since the second order Taylor series expansion of (2.19) in c centered at \bar{c} is proportional to the total variance:

$$J \stackrel{\text{Taylor}}{\approx} \frac{R}{2\bar{c}} \int dV \rho c'^2 \propto \sigma^2 \quad (2.22)$$

Higher moments of c appear for higher order expansions. The second moment of the distribution is identical with the variance. The third moment denotes the skewness, the fourth is called kurtosis, and so on. In summary, the Taylor series of the total negentropy of mixing includes all moments of the distribution, and hence the alternation of all its properties due to the time evolution is captured by the time derivative of J which is simply the negative time derivative of S regarding (2.15). Note that higher moments are also used in “multi-moment advection schemes” (Minoshima et al., 2011).

3 Numerical Treatment of the Transport Equation

3.1 The Kühlungsborn Mechanistic General Circulation Model

For the purpose of the present study a simple general circulation model (GCM) is employed, namely the Kühlungsborn Mechanistic General Circulation Model (KMCM). The prognostic variables are vorticity and divergence describing the horizontal wind field, temperature, and surface pressure. In addition, mass mixing ratios for an arbitrary number of passive tracers can be included. The KMCM's dynamical core is based on the spectral transform method for the horizontal directions combined with the finite-difference scheme introduced by Simmons and Burridge (1981) for the vertical discretization. For the time integration a semi-implicit leapfrog scheme is applied. It is completed by a time filter in order to damp the so called “computational modes” (Asselin, 1972). Additional model descriptions are provided by Becker and Schmitz (2001), Körnich et al. (2003), and Becker (2003). Within the framework of this study, the PE were enhanced by the transport equation (2.7).

3.2 On the Issue of Aliasing

This section considers the aliasing effect and its impact on spectral GCMs.

In spectral GCMs horizontal dependencies of the prognostic variables are represented in terms of spherical harmonics. This representation is exact if the number of harmonics is infinite and the function is continuously differentiable, e.g. shock-like discontinuities must not be involved (Dirichlet condition). As numerical models can only deal with finite, discrete numbers, the transformation is always associated with a truncation error causing aliasing.

If the function is only continuous, or even discontinuous, then the series of spherical harmonics only converges piecewise, but no longer uniformly. This behavior gives rise to ringing and is called Gibbs phenomenon. Ringing has to be distinguished

3 Numerical Treatment of the Transport Equation

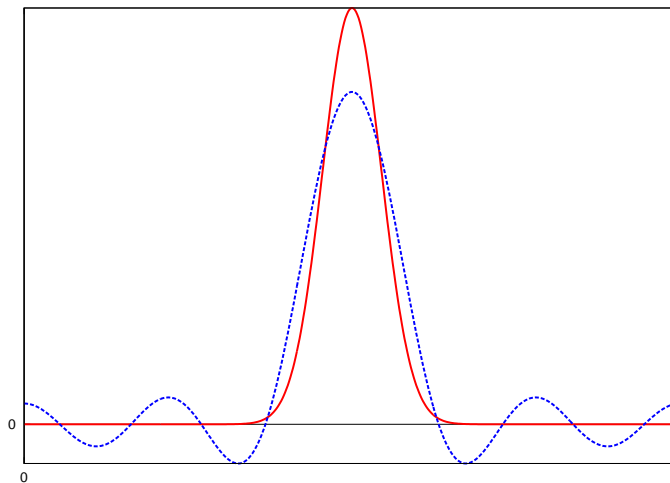


Figure 3.1: A Gaussian curve (solid red line) represented by a Fourier series (dashed blue line) truncated by wave number 4. Note the occurrence of negative values.

from aliasing. The aliasing effect due to the truncation error is shown in figure 3.1 schematically. It can be interpreted as a loss of information due to the spectral transformation.

The major benefits of the spectral method solving the transport equation (2.7) are: First the conservation of mass, and second the exact (according to the machine accuracy) reproduction of the linear terms in the time tendency since the first and second horizontal derivative provides the eigen values of the spherical harmonics. The nonlinear terms must be inversely transformed and computed on the grid. This can cause nonlinear numerical instabilities (see Randall (2004) section 10) called aliasing errors. Although the transport equation is linear in c , aliasing errors can still occur since the coefficients of the derivatives, namely the wind velocity and the diffusion coefficient, are spatially and temporarily variable and hence associated with aliasing errors themselves. Even with a proper spectral representation of the initial distribution, aliasing errors can grow during the time integration. That does not affect only the horizontal evolution, but the vertical as well, because aliasing errors generally occur when formations of short wave-lengths sampled on a discrete grid are misinterpreted due to strong gradients as longer wave-length oscillations. In addition, aliasing also affects GCMs with finite-differencing schemes in all dimensions. In conclusion, the truncation of the spectral representation, as well as

nonlinearities or dependent coefficients give rise to aliasing.

Monotonicity and sign preservation are very important qualities of numerical models. Therefore, it is worth to explore aliasing as it violates both these constraints. The representation of a positive function by spherical harmonics can yield negative values as illustrated in figure 3.1. This becomes an issue if the considered variable, in our case the mass mixing ratio, is supposed to be positive. Negative mass mixing ratios are obviously unphysical. Furthermore, the occurrence of ripples due to the transformation provides new spurious extrema destroying the monotonicity. But the strongest argument for the need of preventing aliasing lies within the total entropy of mixing. Apparently, the spectral transformation causes a loss of entropy, which seems to be counterintuitive as a loss of information due to the truncation is supposed to produce entropy. That may be a logical conclusion from the point of view of the Shannon entropy. But actually the spectral transformation gains a higher state of order in the system, because the transformation reduces the degree of freedom of the function and consequently entropy is lost. This is associated with the destruction of monotonicity mentioned above. But the more convincing impact of aliasing on the entropy is that it is no longer defined for negative mass mixing ratios referencing to equation (2.11) since the logarithm does not exist for negative values.

Common GCMs deal quite differently with the aliasing issue. Some accept negative concentrations as an uncertainty, e.g. GISS ModelE (Schmidt and Coauthors, 2006). Others use additional sign preserving transport schemes, like the semi-Lagrangian, e.g. CAM3 (Collins et al., 2004) and ECHAM5 (Roeckner et al., 2006), which are driven by the spectral velocity field, accepting that it is probably computational expensive. However, Shepherd (2007) argues for spectral tracer advection if a spectral dynamical core is used, because numerical consistency of dynamics and transport is most important. This approach is based on the work of Jöckel (2001) who mentioned that a grid-to-grid transformation (as necessary in semi-Lagrangian schemes) is in general associated with a loss of information due to averaging between the grid cells and therefore artificial diffusive. Especially for long-term tracer transport in the stratosphere artificial diffusion can play a crucial role and can cause a bias in the simulations (Shepherd, 2007).

3 Numerical Treatment of the Transport Equation

Based on the considerations, we develop a numerical transport scheme that deals with the aliasing issue in a sophisticated manner. Since aliasing is immanent in spectral models, at least the problem of negative concentrations has to be fixed.

3.3 A Function of Representation for Positive Definite Mixing Ratios

We introduce a new function of representation for tracer that ensures positive definite mass mixing ratios. In order to show the demands for such a function, we consider the transport equation (2.7), insert a functional \tilde{c} , and replace c by $c[\tilde{c}]$:

$$\partial_t \tilde{c} + \mathbf{v} \cdot \nabla \tilde{c} = \frac{1}{\rho} \nabla \cdot (\rho K \nabla \tilde{c}) + K (\nabla \tilde{c})^2 \frac{d^2 c}{d\tilde{c}^2} \left(\frac{dc}{d\tilde{c}} \right)^{-1} \quad (3.1)$$

Here, c should be treated as the inverse of the functional \tilde{c} . Therefore, \tilde{c} must be bijective and continuous. As we can see, the second term on the right hand side of equation (3.1) includes the first and second derivative of c with respect to \tilde{c} . Using the differentiation formula for inverse functions we further must claim \tilde{c} to be at least twice continuously differentiable. Additionally, any smooth function fulfills these constraints. Scinocca et al. (2008) described a related method for spectral moisture advection with a piecewise continuous “hybrid” variable proposed by Boer (1995) for the GCM of CCCma called AGCM3 which does not fulfill the aforementioned requirements. But in order to derive \tilde{c} we use an analog approach. Consider the identity:

$$c \equiv c_0 \exp\{\ln(c/c_0)\} \quad (3.2)$$

Here, c is positive anyway. We now substitute the exponent by a first order Taylor series expansion of the logarithm centered at one, hence $\ln(c/c_0) \approx c/c_0 - 1$. Replacing c on the right hand side of equation (3.2) with \tilde{c} leads to

$$\boxed{c = c_0 \exp\{\tilde{c}/c_0 - 1\}}. \quad (3.3)$$

This definition for the function of representation guarantees positive concentrations and is adequate to the requirements since it is a smooth function. Only a few

3.3 A Function of Representation for Positive Definite Mixing Ratios

properties will be discussed: We compute the variation of c .

$$\delta c = \delta \tilde{c} \exp\{\tilde{c}/c_0 - 1\} \quad (3.4)$$

When $\tilde{c} \approx c_0$, the exponent vanishes and the function is approximately linear. In case of $\tilde{c} > c_0$, the variation of c increases exponentially with \tilde{c} , i.e. when using \tilde{c} as a prognostic variable that is represented by spherical harmonics and vertically discretized, the corresponding numerical resolution of c is decreased. On the other hand, the numerical resolution of c increases for $\tilde{c} < c_0$. This is a big advantage taking the typical evolution of an atmospheric long-term tracer, like CO_2 or SF_6 , into account. It starts with high mixing ratio at the earth's surface, getting rapidly mixed in the troposphere, and enters the stratosphere through the equatorial tropopause with a small concentration. Therefore, it is necessary to choose a typical mixing ratio c_0 for every tracer to minimize numerical errors.

The spectral method and the vertical discretization in KMCM are constructed in a way that it conserves the total tracer mass when solving the linear transport equation (2.7) with c as the prognostic variable. Now, the function of representation \tilde{c} is the prognostic variable instead of c . The corresponding non-linear partial differential equation treated in KMCM is

$$\partial_t \tilde{c} = -\mathbf{v} \cdot \nabla \tilde{c} + \frac{1}{\rho} \nabla \cdot (\rho K \nabla \tilde{c}) + \frac{K}{c_0} (\nabla \tilde{c})^2 = f . \quad (3.5)$$

In order to solve the equation with the spectral method, \tilde{c} is expanded in series of spherical harmonics Y_{nm} with wavenumbers n and m for the horizontal coordinates, longitude λ and latitude ϕ . The vertical discretization uses a terrain following hybrid coordinate numerically represented by layers l (Becker, 2003).

$$\tilde{c}_l(\lambda, \Phi, t) = \sum_{nm} \tilde{c}_{lnm}(t) Y_{nm}(\lambda, \Phi) \quad (3.6)$$

Applying Galerkin's method the model equation can be written as:

$$\dot{\tilde{c}}_{lnm} = \int d\Omega f_l Y_{nm} \quad (3.7)$$

3 Numerical Treatment of the Transport Equation

Here, Ω denotes the solid angle. The horizontal derivatives in f_l can be computed in spectral space by using the analytical derivations of the spectral representation and taking advantage of the orthogonality of the spherical harmonics:

$$\int d\Omega Y_{nm} Y_{n'm'} = \delta_{nn'} \delta_{mm'} \quad (3.8)$$

All other terms of f_l have to be computed on the grid. Equation (3.7) is time integrated with the semi-implicit leapfrog scheme. Assuming that the non-linearity of f_l is computed with high accuracy, the global integral of \tilde{c} is now the conserved measure. But no longer is it the total tracer mass. Hence, the scheme loses or produces tracer mass during the time evolution.

The method can be tuned by adjusting c_0 during a simulation trying to decrease the impact of the mass defect. There are several disadvantages of this approach: One needs to compute c_0 depending on the time and further it is nearly impossible to keep the mass constant in a long-term simulation. Therefore, a mass correction is necessary.

3.4 A Mass Correction for General Circulation Models

It is crucial that the total mass of a tracer is conserved in time, especially for long-term model experiments, e.g. simulating the “age of air”. The purpose of this section is to introduce a very general method for a tracer mass correction that allows us to use the new function of representation for the mixing ratio of a tracer, particularly for long-term simulations. Note that such mass correction must be numerically efficient. We must take into account that an expensive, ineffective method would destroy the benefits of the new function of representation in combination with the spectral transform method.

Mass corrections or mass fixer or mass restorations, alternatively, are closely related to “hole filler”. The latter are used to fill holes of negative mixing ratios with material borrowed from points of positive ones. An extended overview about “hole filler” is given by Rood (1987). With the function of representation introduced in section 3.3 the mixing ratio is positive definite by definition.

A common mass correction algorithm is the mass fixer documented in Collins et al.

3.4 A Mass Correction for General Circulation Models

(2004) for CAM3. In their model it is applied along with a semi-Lagrangian transport scheme. A related approach to a mass restoration like the one in this work is presented by Moorthi et al. (1995) with regard to the surface pressure. The basic idea of the mass correction proposed in this study is to compute the mass defect every time step and to redistribute it in a manner that the total mass converges to its initial value. This can formally be described by the following equation:

$$c_{new}(\mathbf{r}, t) = \kappa(t) w[c_{old}(\mathbf{r}, t)] \quad (3.9)$$

Here, c_{old} denotes the tracer concentration associated with a mass defect and c_{new} the corrected one at time t and at point \mathbf{r} representing longitude, latitude and altitude. Furthermore, we must specify a weight function w depending on c_{old} . It has to be chosen in a way that the mass correction is most effective at points where the greatest mass defects are expected. And it also controls the strength of the change caused by the correction. Note that the weight function gives rise to a spurious change in the entropy of mixing as it refers to a mass transfer.

In order to ensure conservation of the total mass the factor κ has to be derived with respect to the fact that w is meant to be arbitrary. We define the current uncorrected total mass M_{old} at model time t via the volume integral over the whole atmosphere:

$$M_{old}(t) = \int dV \rho(\mathbf{r}, t) c_{old}(\mathbf{r}, t) \quad (3.10)$$

The new total mass after correction is presumed as

$$M_{new} = M_{old} + \zeta (M_0 - M_{old}) \quad (3.11)$$

Here, M_0 denotes the total mass of the initial concentration. If there are neither sources nor sinks, one needs to compute M_0 only once. Otherwise, i.e. for reactive tracer, it is necessary to calculate M_0 every time step from sources and sinks, e.g. condensation and precipitation rates when considering water vapor as a tracer. The factor ζ is inserted in (3.11) as a control parameter, i.e. ζ is the parameter of mightiness for the mass correction. It corresponds to the number of time steps until M_{old} is forced to be equal to M_0 again. For $\zeta = 0$ no changes will be achieved and

3 Numerical Treatment of the Transport Equation

for $\zeta = 1$ the maximum effect will occur. Note that a strong effect may give rise to numerical instabilities. Using (3.11) the coefficient κ can be written as:

$$\kappa = \frac{M_{old} + \zeta (M_0 - M_{old})}{\int dV \rho w} \quad (3.12)$$

In addition to the choice of w , it is crucial to take account of the representation function \tilde{c} . Actually, we must write $w = w[c_0 \exp\{\tilde{c}_{old}(\mathbf{r}, t)/c_0 - 1\}]$. For integrating w (see denominator of equation (3.12)) one has to transform \tilde{c} from its spectral into its grid point representation, and vice versa after the mass correction has been applied. Thus, truncation errors can increase and consequently the benefits of the mass correction can vanish when w is selected in an insufficient manner. Moreover, in case of a careless choice of w it is also possible to create an amount of tracer concentration at points where the concentration should be close to zero, like a sort of “teleportation”.

We introduce a very intuitive way to choose w that provides convenient but nevertheless efficient results. We choose:

$$w[c_{old}] = c_{old} \quad (3.13)$$

This implicates that the mass defect is allocated uniformly over the atmosphere weighted by the concentration itself, i.e. the higher the mixing ratio at one point, the more it will be corrected. Furthermore, (3.13) prevents the effect of “teleportation” because at points with concentration near zero the mass correction has almost no effect. This is related to the constraint of monotonicity: Multiplying a monotone function by a constant factor does not change its characteristics. Thus, the proposed mass correction is monotonicity preserving.

Replacing c by the new prognostic variable \tilde{c} yields:

$$\tilde{c}_{new}(\mathbf{r}, t) = c_0 \ln \kappa(t) + \tilde{c}_{old}(\mathbf{r}, t) \quad (3.14)$$

We now expand \tilde{c} in series of spherical harmonics according to (3.6) and take advantage of the orthogonality of Y_{nm} (condition (3.8)). We obtain the mass correction

3.4 A Mass Correction for General Circulation Models

for the spectral amplitudes of \tilde{c} on each layer,

$$\tilde{c}_{new,100}(t) = 2\sqrt{\pi} c_0 \ln \kappa(t) + \tilde{c}_{old,100}(t) \quad (3.15)$$

with

$$\kappa = 1 + \zeta (M_0/M_{old} - 1) . \quad (3.16)$$

The obvious benefit of this formula is that only one spectral coefficient, namely the mean value of \tilde{c} on each layer, has to be changed. No additional spectral transformations need to be done. Furthermore, we can even simplify this method by considering κ again: As we require the effect of the correction to be slight for numerical stability, we can assume the total mass M_{old} to vary in a small range about M_0 . Therefore, it is appropriate to expand the logarithm of κ to a first order Taylor series. This leads us to the final expression which is implemented in KMCM for the mass correction:

$$\boxed{\tilde{c}_{new,100} = 2\sqrt{\pi} c_0 \zeta \left(\frac{M_0}{M_{old}} - 1 \right) + \tilde{c}_{old,100}} \quad (3.17)$$

Both mass corrections with and without Taylor approximation for κ have been tested in KMCM. The results are the same and hence the approximation proves to be appropriate.

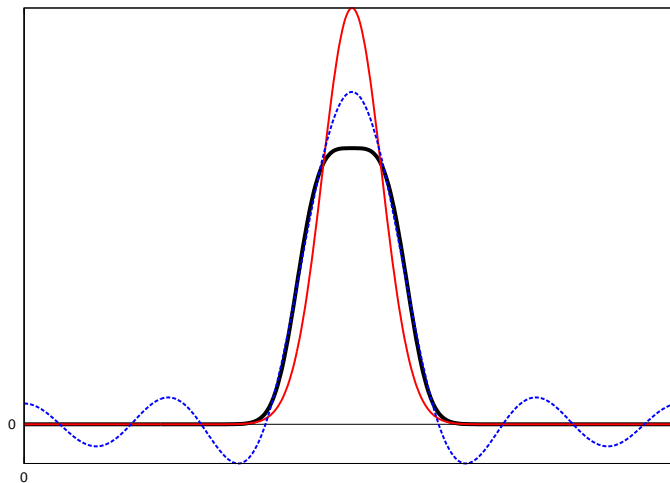


Figure 3.2: A Gaussian curve (solid red line). Its representation by a Fourier series (dashed blue line). And the Fourier series of its mass corrected function of representation (thick black line). All truncated by wave number 4. Note the disappearance of aliasing by the mass corrected function of representation.

In addition to the higher numerical resolution of the scheme for small mixing ratios (see section 3.3), strong gradients are also better represented by the function of representation in combination with the mass correction as illustrated in figure 3.2. The proposed scheme can better deal with strong gradients without the occurrence of aliasing due to the truncation of the Fourier series than the ordinary scheme. Although the initial function (solid red line in figure 3.2) is considerably deformed by the fast truncation of the Fourier series of its mass corrected function of representation (thick black line in figure 3.2), it is worth noting that the monotonicity and the sign is preserved. This may be an advantage as the issue of sharp gradients in spectral GCMs is often criticized (Williamson and Rasch, 1994).

4 Validating the scheme

The previous section has proposed a method for tracer transport in a spectral GCM including a new function of representation for a positive mixing ratio and a mass correction. In order to proof the numerical consistency, conservation, and monotonicity of the derived method, several tests will be performed. The aim of these tests is to show the functionality as well as finding the lower and upper limits of parameters the numerics can still deal with. We can distinguish two kinds of parameters: First, the set of control parameters, namely ζ and c_0 . Second, the set of the physical parameters which are the coefficients of the transport equation, i.e. the velocity field and the diffusion coefficients. The influence on the numerics by the choice of ζ and c_0 will be discussed in section 4.5 and 4.4.

For the physical parameters we use a benchmark deformational flow test based on the idea of making the analytical solution available at the end of the simulation by constructing a flow that leads back to the initial condition. Then, the resulting mixing ratio can be compared directly with its initial distribution. Apparently, the diffusion coefficient must be set to zero, otherwise the tracer would be mixed irreversibly and the analytical solution would no longer apply.

The basic idea is to provide a flow deforming the tracer as challenging as possible along non-trivial trajectories for a prescribed time $T/2$. Therefore, no analytical solutions are accessible during this deformation. By reaching $T/2$ the flow turns into its opposite direction such that after time T every air parcel returns to its starting point (Nair and Lauritzen, 2010). One can derive a wind field fulfilling these qualities simply by multiplying an arbitrary field by $\cos(\pi t/T)$ as first proposed by LeVeque (1996).

We provide two different deformational flow test cases of this kind: A non-divergent flow with only horizontal transport in section 4.2 and a purely divergent flow with only meridional and vertical transport in section 4.3 in order to test the different numerical methods used for vertical and horizontal transport. Numerical

4 Validating the scheme

errors are monitored by the total mass and the total entropy of mixing (see section 2).

4.1 Initial Condition

The initial mixing ratio for the experiments is generated by Gaussian curves in all three dimensions completed by an offset value due to the requirement that c is not allowed to be zero anywhere and finally filtered with a window function avoiding discontinuities at the poles:

$$c(t_0) = c_{off} + c_{ini} \cos^{1/4}(\phi) e^{-G^2} \quad (4.1)$$

$$G^2 = \frac{(\phi - \phi_0)^2}{4\sigma_\phi^2} + \frac{(\lambda - \lambda_0)^2}{4\sigma_\lambda^2} + \frac{(p - p_0)^2}{4\sigma_p^2} \quad (4.2)$$

Both the non-divergent and the purely divergent test runs are defined by a set of parameters listed in the table below (see also figure 4.1).

parameter description	symbol	non-divergent	purely divergent
center of altitudinal Gaussian curve	p_0	800 hPa	700 hPa
width of altitudinal Gaussian curve	σ_p	150 hPa	100 hPa
center of meridional Gaussian curve	ϕ_0	0°	0°
width of meridional Gaussian curve	σ_ϕ	11.459°	5.730°
center of zonal Gaussian curve	λ_0	180°	180°
width of zonal Gaussian curve	σ_λ	11.459°	5.730°
maximum mixing ratio	c_{ini}	1	1
offset in mixing ratio	c_{off}	0.001	0.001

Figure 4.1: Initial parameters for the benchmarks

4.2 Non-Divergent Flow

The prognostic variables in the KMCM for the three-dimensional velocity field are the horizontal vorticity ξ as well as the horizontal divergence D in combination with the surface pressure p_s . In a non-divergent flow only the vorticity plays a role. Therefore, D is set to zero and p_s is set to constant ($p_s = p_{00}$ with $p_{00} = 1013 \text{ hPa}$).

4.3 Purely Divergent Flow

Since the horizontal stream function Ψ and the horizontal vorticity are connected due to

$$\xi = \nabla^2 \Psi , \quad (4.3)$$

one can use the more intuitive horizontal stream function to design a test flow. Nair and Lauritzen (2010) proposed for a non-divergent, time-dependent wind field:

$$\Psi = k \sin^2(\lambda/2) \cos^2(\phi) \cos(\pi t/T) \quad (4.4)$$

Here, k is an arbitrary factor representing the amplitude of the displacement affecting the tracer. It can be derived as the maximum velocity u_0 scaled by the earth's radius a , i.e. $k = au_0$. For the non-divergent flow case u_0 is set to 600 m s^{-1} , which is obviously not very realistic but challenging instead. The term T is the time period (see section 4) after which the mixing ratio reaches its initial distribution. T is 4 days for all the following simulations. We now expand Ψ in series of spherical harmonics according to (3.6). Since Y_{nm} are eigenfunctions of the horizontal Laplace operator, equation (4.3) can be written in spectral space as:

$$\xi_{nm} = -\frac{n(n+1)}{a^2} \Psi_{nm} \quad (4.5)$$

Additionally, the entire function of Ψ and hence ξ is shifted in zonal direction about $2\pi/3$ for reasons of simplicity in the KMCM. The artificial parameter c_0 is set to one. Whether this is a proper choice will be discussed later.

4.3 Purely Divergent Flow

In the purely divergent flow case only the horizontal divergence plays a role and hence the horizontal vorticity is set to zero and the surface pressure to constant ($p_s = p_{00}$). We propose an analytical formula for the divergence in the following way:

$$D = k(1 - 3 \sin^2(\phi)) \cos(\pi p/p_{00}) \cos(\pi t/T) \quad (4.6)$$

Equation (4.6) is inspired by LeVeque (1996), too. The basic idea is to obtain a kind of a zonally symmetric Hadley cell lifting the tracer up on deforming trajectories

4 Validating the scheme

and bringing it back perfectly by switching from upwelling to downwelling during the period T . For this purpose we must take into account that the mean value of the horizontal divergence must vanish in order to conserve the total mass. In the KMCM as well as in other spectral GCMs, this is associated with the fact that the $(0, 0)$ -component of D is zero. To meet this constraint the meridional dependence (the second factor in (4.6)) is equivalent to the spherical harmonic function $Y_{02}(\lambda, \phi)$. Since the surface pressure is constant in time, the integral of D with respect to the pressure over the whole air column must vanish in order to fulfill the continuity equation (2.3). This explains the choice of the third factor in (4.6). The maximum velocity u_0 is set to 400 m s^{-1} .

4.4 Assessing the Total Entropy of Mixing

In this section the influence of the mass correction on the total entropy of mixing is estimated in order to evaluate the physical and numerical consistency of the mass correction. Since the negentropy of mixing is equivalent to the entropy of mixing and easier to handle, the total negentropy of mixing J is used for this purpose.

Inserting $c_{new} = \kappa c_{old}$ (see section 3.4) into (2.19) yields

$$J_{new} = \kappa J_{old} \tag{4.7}$$

for the mass correction. The parameter κ of (3.16) depends on M_{old} and ζ . Small mass defects and a small ζ give rise to insignificant changes in J due to the mass correction. This is desired because the mass correction is in general unphysical. Therefore, the resolution must be high enough so that the scheme without the mass correction already keeps the tracer mass as constant as possible. Equation (4.7) has to be considered in contrast to

$$M_{new} = \kappa M_{old} \tag{4.8}$$

which follows from definition (3.11). It denotes that the mass correction affects the total tracer mass in exactly the same magnitude as it affects the total negentropy of mixing. Most important is the direction of the change. For a negative mass defect

4.5 Analysis and Results of the Benchmarks

the mass correction must annihilate entropy to give mass back to the system and vice versa. Hence, it is crucial to examine how the entropy is linked to the mass defect for the scheme without mass correction. In particular, for little mass defects and a slender mass correction the scheme is supposed to work with high consistency following Shepherd (2007) who argued for spectral transport schemes in spectral GCMs.

4.5 Analysis and Results of the Benchmarks

This section analyzes the results of the benchmarks. Both experiments, the non-divergent and the purely divergent case, have shown similar characteristics and hence they will be discussed in the same context. As a first result of both benchmarks it must be recognized that the numerical scheme is stable even under these challenging conditions, i.e. deformational flow fields with very strong winds combined with a coarse resolution. Regarding the corresponding analysis by the use of the diagnostic measures we need to keep in mind that the flows are unrealistic because of the idealized “laboratory”-like conditions. Tests under more realistic circumstances (the KMCM is tuned as described in Becker (2003)) has proven to be much less challenging for the scheme.

4 Validating the scheme

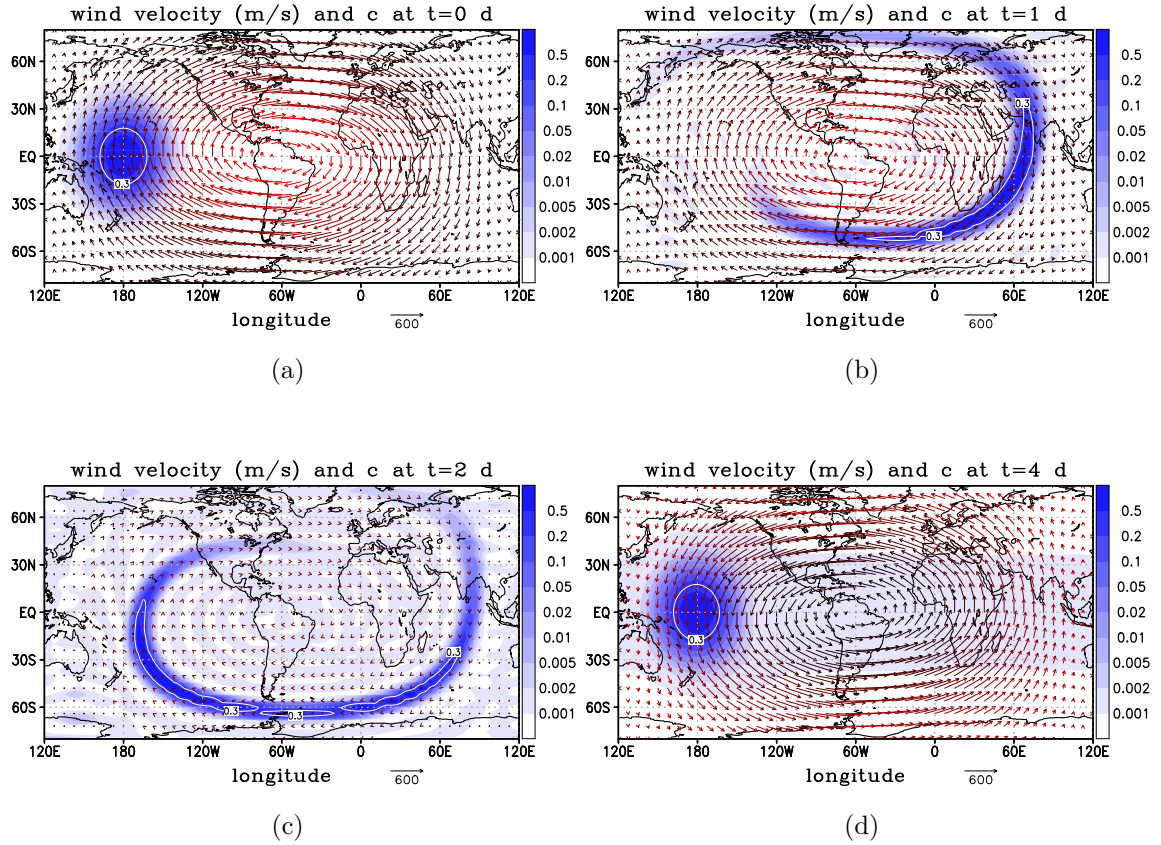


Figure 4.2: Time evolution of a tracer in a non-divergent flow benchmark test (see section 4.2). (a) Initial distribution, (b) after $T/4 = 1$ d, (c) after $T/2 = 2$ d, when the velocity field reverses, and (d) after $T = 4$ d, when the tracer field is expected to match with the initial distribution. The mass correction is adjusted with $\zeta = 0.2$. Spectral resolution T31 and 30 vertical levels. The mass mixing ratio is plotted using a logarithmic color scale at a pressure level of 800 hPa. Wind field vectors are colored with increasing values of the horizontal stream function from black to red. The mixing ratio of 0.3 is indicated by a white contour in each panel in order to highlight any aliasing effects.

4.5 Analysis and Results of the Benchmarks

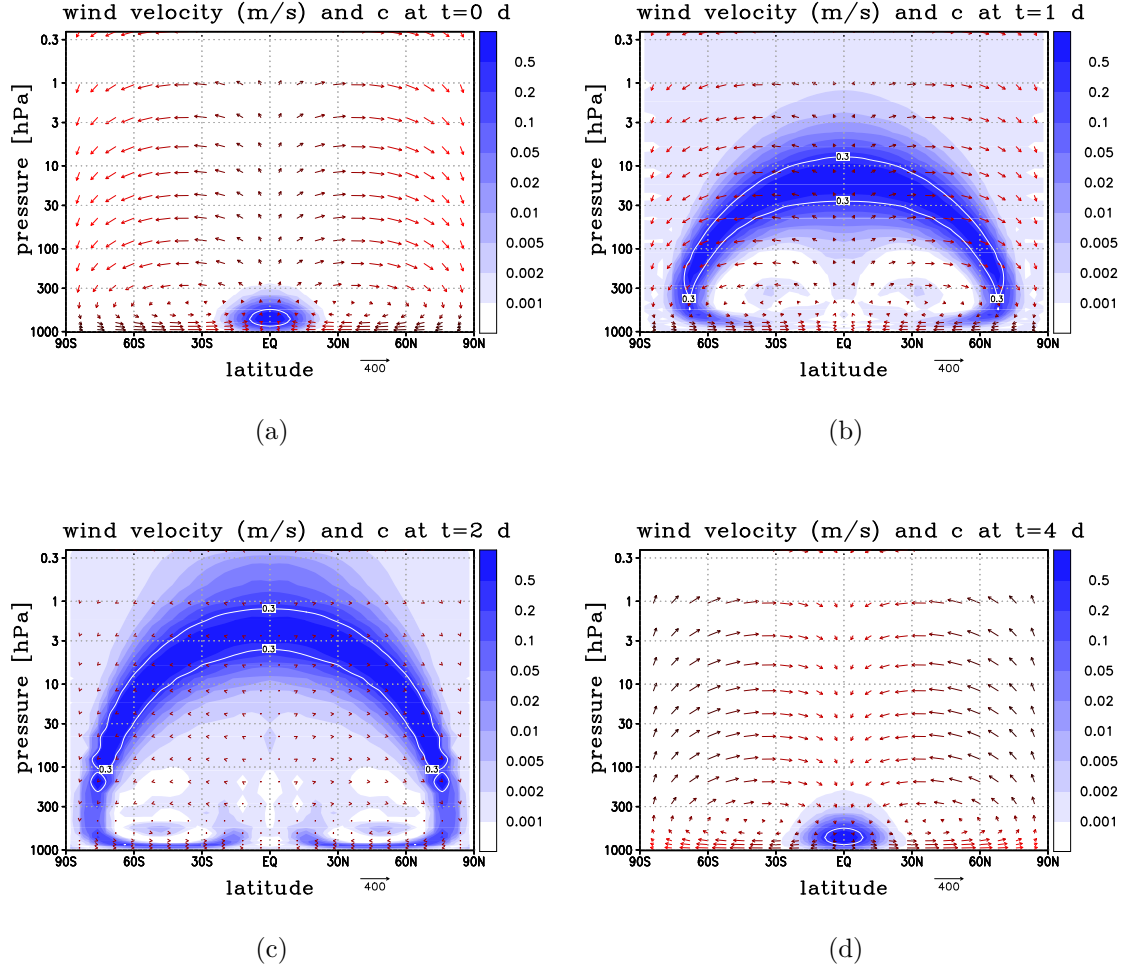


Figure 4.3: Time evolution of a tracer in a purely divergent flow benchmark test (see section 4.3). (a) Initial distribution, (b) after $T/4 = 1 d$, (c) after $T/2 = 2 d$, when the velocity field reverses, and (d) after $T = 4 d$, when the tracer field is expected to match with the initial distribution. The mass correction is adjusted with $\zeta = 0.2$. Spectral resolution T31 and 30 vertical levels. The mass mixing ratio is plotted using a logarithmic color scale at a longitude of 180° . Wind field vectors are colored with increasing values of the horizontal velocity potential from black to red. The mixing ratio of 0.3 is indicated by a white contour in each panel in order to highlight any aliasing effects.

4 Validating the scheme

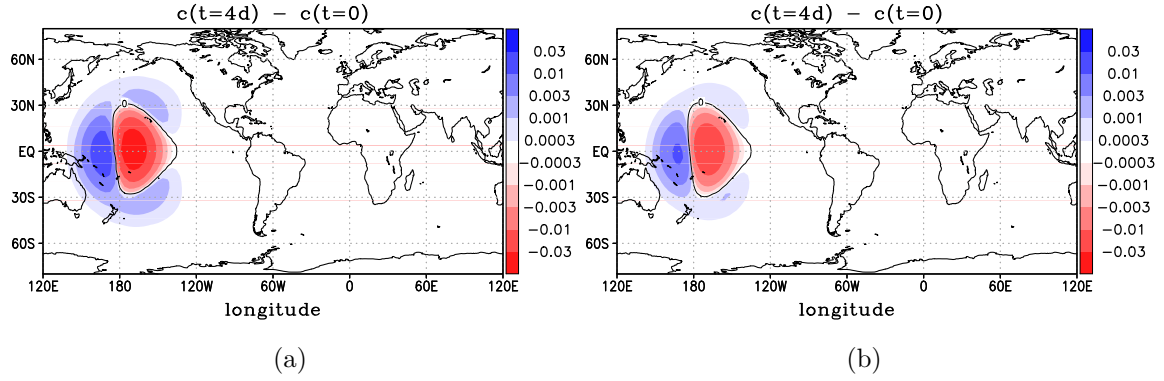


Figure 4.4: Dependence on resolution in the none-divergent flow benchmark test. Difference between the final and initial mixing ratio for T31 (a) and T42 (b) spectral resolution. These differences represent the numerical error in the two simulations (see section 4).

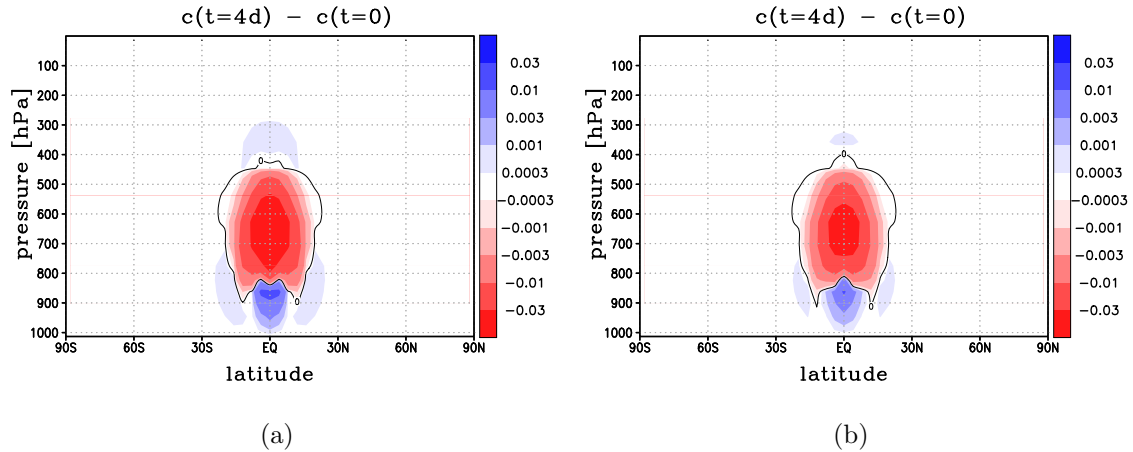


Figure 4.5: Dependence on resolution in the purely divergent flow benchmark test. Difference between the final and initial mixing ratio for T31 (a) and T42 (b) spectral resolution. These differences represent the numerical error in the two simulations (see section 4).

4.5 Analysis and Results of the Benchmarks

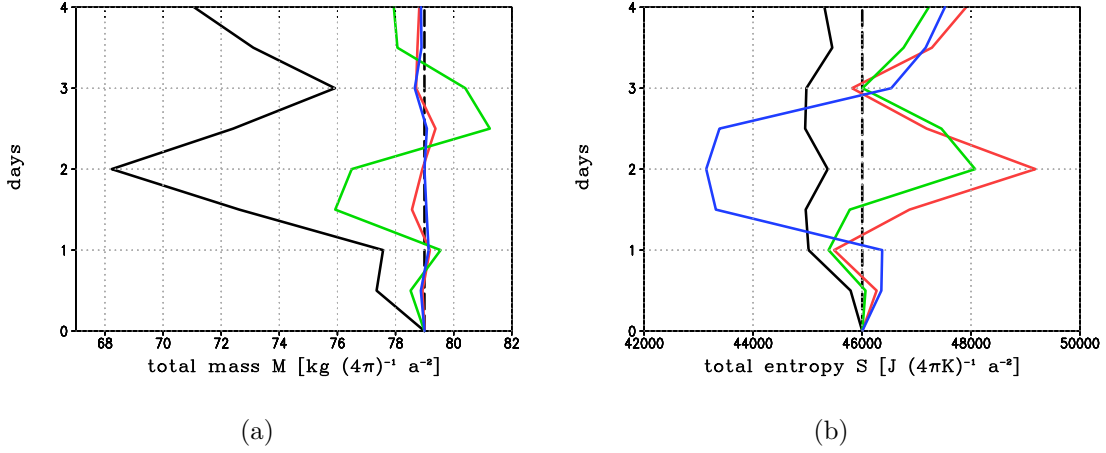


Figure 4.6: Total tracer mass (a) and total entropy of mixing (b) as functions of time in the non-divergent flow benchmark test: Black solid line: Without mass correction, T31 spectral resolution; Green solid line: With mass correction ($\zeta = 0.02$), T31; Red solid line: With mass correction ($\zeta = 0.2$), T31; Blue solid line: With mass correction ($\zeta = 0.2$), T42; Dashed black line: Initial values for total mass and total entropy of mixing.

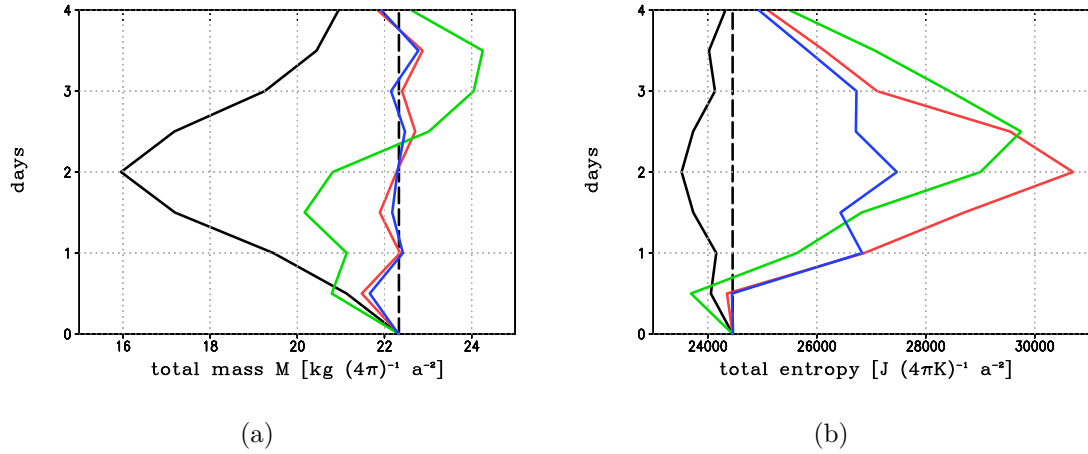


Figure 4.7: Total tracer mass (a) and total entropy of mixing (b) as functions of time in the purely divergent flow benchmark test. Black solid line: Without mass correction, T31 spectral resolution; Green solid line: With mass correction ($\zeta = 0.02$), T31; Red solid line: With mass correction ($\zeta = 0.2$), T31; Blue solid line: With mass correction ($\zeta = 0.2$), T42; Dashed black line: Initial values for total mass and total entropy of mixing.

4 Validating the scheme

The non-divergent and the purely divergent deformational flow test are shown in figure 4.2 and 4.3. The tracer starts with its initial distribution in figure 4.2(a) and 4.3(a) and gets maximally deformed by the flow field in figure 4.2(c) and 4.3(c) where the wind direction is turning. The tracer returns in figure 4.2(d) and 4.3(d) where it should match with the initial distribution. How it matches, can be seen in figure 4.4 and 4.5. Here, the difference between final and initial distribution is illustrated. Finally, figure 4.6 and 4.7 show the time dependence of total tracer mass and total entropy of mixing.

Within the settings of the non-divergent flow the impact on the numerical stability by the choice of c_0 was tested by varying c_0 in a range of several magnitudes ($10^{-5} \leq c_0 \leq 10^6$). The differences among the results (not shown) were insignificantly small. From the lowest to the largest c_0 the maximum peaks of c varied by less than 1%. In conclusion, the choice $c_0 = 1$ is appropriate for a wide spectrum of applications.

In the figures 4.2(c) and 4.3(c) can be seen that weak aliasing errors with regard to section 3.2 still occur when considering the contour of a mixing ratio of 0.3 and the swinging background noise which is highlighted by the logarithmic scaling of the color scheme. But nevertheless, this effect seems to be small as it does not affect significantly the final distribution. Note that spectral GCMs are always contaminated with aliasing errors.

Figure 4.4 and 4.5 illustrate the relation between numerical errors and resolution. The difference between the final and initial distribution is at most 3% for a T31 resolution. Furthermore, the asymmetrical distribution of the error can be interpreted as a phase-speed error. Nair and Lauritzen (2010) noticed that phase errors can cancel when the flow reverses on the same trajectories and hence a zonal background flow was introduced. We tested both benchmark cases additionally with an underlying solid-body rotation with a self-evident period of 4 days in order to prevent this cancellation, but no significant differences in the numerical errors occurred. Therefore, the phase-speed errors are seemingly immanent. However, with increasing resolution the numerical error decreases. For a T42 resolution the numerical error is about, or even lower, than 1% at the peak.

Without the mass correction the scheme is still stable, but the total mass is far

4.5 Analysis and Results of the Benchmarks

from being constant. On the other hand the total entropy of mixing is approximately constant as shown in figure 4.6(b) and 4.7(b) (solid black lines). With respect to section 4.4, where we already mentioned the importance of the direction of the change in entropy, we see from figure 4.6 and 4.7 that the scheme without mass correction loses total entropy of mixing when losing total mass. Apparently, the mass defect behaves like a constant sink term in the transport equation. Inserting such an artificial sink term in (2.12) it is easy to show that it annihilates entropy. The mass correction works vice versa, i.e. if the uncorrected scheme loses entropy because it loses mass, then the mass correction annihilates further entropy by producing mass.

Aliasing errors also reduce entropy whereas numerical diffusion produces entropy. We argue that the slightly varying total entropy of mixing of the scheme without mass correction in figure 4.6(b) and 4.7(b) (solid black line) is dominated by the mass defect and the numerical diffusion balancing each other whereas aliasing plays a minor role. The perfect numerical transport scheme would keep total mass as well as total entropy constant. As this perfect scheme does not exist, we have to find a compromise how to adjust the mass correction to satisfy the constraints of total mass and total entropy conservation as good as possible.

As noted in section 3.4, the parameter ζ controls the strength of the mass correction. It must be in the interval between zero and one. If ζ is set to one, the mass will be corrected from one time step to the next to its absolute initial value and the impact on the entropy will be strongest. But is that necessary? Actually, the mass correction can ensure long-term mass conservation by small adjustments to the total mass. In addition, the mass correction has a slight unphysical influence on the entire transport as it replaces tracer mass. So we want to allow the total mass to vary in a small range about M_0 , but to converge to M_0 with time because the spurious transport due to the mass correction must be small in comparison to the true transport. The red and the blue lines in figure 4.6 and 4.7 reveal the influence of ζ on the transport. For a small ζ (green lines) the total mass fluctuates significantly while the variations of the total entropy of mixing are small. This should be contrasted to the red lines. Here, the parameter ζ is 10 times stronger while using the same resolution. In this case, total mass variations are reduced whereas those of the total entropy of mixing are increased. For the same ζ but with a higher resolution of T42

4 *Validating the scheme*

(blue lines) mass conservation is nearly fulfilled and the influence on the entropy is further decreased. But as a higher resolution causes a smaller mass defect, it is supposed to apply a smaller ζ . This is supported by the constraint that a physically consistent transport is rated higher than a perfect total mass conservation at all times. Another argument is provided by the demand for a compromise mentioned above.

Additionally, regarding figure 4.6(b) and 4.7(b) (green, red, and blue lines) the production of entropy of mixing is on average positive. This suggests that the scheme with mass correction is somewhat numerically diffusive. Without any mass correction the scheme loses entropy because of the mass defect. It gains entropy due to numerical diffusion if we assume that aliasing has no significant influence. The resulting balance tends slightly to the mass defect. Turning on the mass correction the mass defect vanishes while numerical diffusion still generates entropy. In section 4.4 we stated that the mass correction annihilates entropy. But since the mass correction is monotonicity preserving, this annihilation must mimic a kind of anti-diffusion. This anti-diffusion balances the numerical diffusion. But the latter still dominates. As long as the resulting numerical diffusion is small in comparison to a realistic, natural diffusion applied in simulations, this anti-diffusion can be considered as a beneficial secondary effect.

5 Conclusion

5.1 Summary

A new mass and sign preserving tracer transport scheme for spectral atmospheric general circulation models has been introduced and validated by benchmark test cases. The tests have shown a high stability of the scheme even for flows with strong shear combined with a coarse resolution.

A function of representation for positive definite tracer mass mixing ratios has been developed. This function depends on an adjustable parameter which is representative of a typical mass mixing ratio. The experiments have shown that the numerical results are hardly sensitive to this parameter. For the sake of simplicity we have proposed to set it equal one.

In order to achieve mass conservation a mass correction has been derived which is computationally very efficient in combination with the function of representation since it affects only the zeroth spectral component of the latter. The mass correction is adjustable by a parameter which controls the mightiness of the correction. This control parameter should be small such that the spurious transport due to the mass correction is negligible in comparison to the physical transport. The benchmark tests have suggested that the choice of this parameter should depend also on the resolution. The higher the resolution, the weaker the mass defect. Hence, for higher resolution the control parameter can be smaller. We propose even for coarse resolution to choose the control parameter of the mass correction not greater than 0.2.

For the purpose of validating the benchmark results the concept of the entropy of mixing has been adopted to the issue of tracer transport. We state that the total entropy of mixing can be used as a diagnostic quantity for the physical consistency of the transport scheme. Since the total entropy of mixing is conserved with regard to advection (only diffusion can alter the total entropy of mixing of a passive tracer),

5 Conclusion

it is possible to measure the impact of spurious numerical effects by monitoring it. Hence, the total tracer mass and additionally the total entropy of mixing has been used to evaluate the transport scheme. With the help of the entropy of mixing we have found that the proposed scheme is less artificially diffusive than the ordinary spectral transport method. Furthermore, the new scheme can better deal with strong spatial gradients before aliasing occurs.

5.2 Implications and Future Tasks

The purpose of this section is to discuss some further ideas and conceptual implications of this study. With regard to section 3.3 one may ask for an equivalence of the function of representation to other existing theories. Within the field of information theory the so called self-information function I is well known (Shannon, 1948). It denotes the “surprisal” of the occurrence of a statistical event. Its expected value with respect to the profile (here c) is the entropy or rather the Shannon entropy which is related to the entropy of mixing. Minoshima et al. (2011) adopted this concept for numerical advection schemes. In the nomenclature of the present work they defined:

$$s = c I[c] \tag{5.1}$$

Comparing (5.1) with the definition of s in (2.20) yields:

$$I = -R \ln c \tag{5.2}$$

When we derive the inverse of (3.3) using $c_0 = 1$, we obtain the function of representation.

$$\tilde{c} = \ln c + 1 \tag{5.3}$$

Apparently, I and \tilde{c} are linearly dependent in c , i.e. it should not make a difference, if we use the one or the other as the prognostic spectral variable. Note that the function of representation is a kind of self-information function.

But what does this mean in the context of transport? If the self-information in information theory denotes the “surprise” of the outcome of a signal channel in time with the knowledge of all outcomes before, then the self-information with

5.2 Implications and Future Tasks

respect to transport must be the “surprise” of a mixing ratio at a certain point with the knowledge about all the other points. As the numerical treatment of the prognostic variables in the KMCM is designed in order to achieve conservation, we can reason that the self-information is conserved when the function of representation is employed. Thus, in terms of information theory the global information content (in contrast to the global entropy) remains constant in time.

The future tasks with the KMCM and the transport algorithm will be to estimate the “age of air” and to simulate the transport of water vapor and other chemical species. Therefore, it is necessary to implement sources and sinks in the transport scheme. These additional terms depend on time and location as they represent the production and reduction rates of the constituents, e.g. condensation of water vapor in clouds. For this purpose we propose to use both the total mass and the total negentropy of mixing as additional prognostic variables. For each constituent this denotes only two additional components and hence it is hardly further computationally expensive since total mass and total negentropy of mixing should be computed to monitor the performance of the transport scheme anyway.

In order to assure global conservation of mass and negentropy, we propose to use a mass and negentropy correction:

1. Execute the time stepping on the mixing ratio, the prognostic total mass, and the prognostic total negentropy of mixing.
2. Compute the actual total mass with (3.10) and correct it with the proposed mass correction:

$$c_{new} = \kappa C_{old} \tag{5.4}$$

Instead of M_0 the new prognostic total mass is used to compute κ .

3. Compute the actual total negentropy of mixing with (2.19) and correct it according to a new approach:

$$c_{newest} = c_{new} - \mu \nabla^2 c_{new} \tag{5.5}$$

The parameter μ is a kind of an anti-diffusion coefficient and represents the defect between numerical and physical diffusion. We may derive μ from the

5 Conclusion

new prognostic total negentropy of mixing with an approach similar to (3.11).

Note that (5.5) is closely related to “flux-corrected transport (FCT)” (Boris and Book, 1973). But instead of deriving an anti-diffusion from higher order schemes we propose to compute it explicitly from the total negentropy of mixing. Furthermore, it must be acknowledged that FCT computes the flux for every fluid parcel whereas the proposed negentropy correction is an approximation on the globe. A real FCT scheme can be provided by computing the anti-diffusive flux from (2.20).

Bibliography

- R. Asselin. Frequency filter for time integration. *Mon. Wea. Rev.*, 100:487–490, 1972. doi: 10.1175/1520-0493(1972)100<0487:FFFTI>2.3.CO;2.
- E. Becker. *Energetics of turbulent momentum diffusion and gravity wave breakdown in general circulation models of the atmosphere*. Habilitation, University of Rostock, 2003. 86pp.
- E. Becker and G. Schmitz. Interaction between extratropical stationary waves and the zonal mean circulation. *J. Atmos. Sci.*, 58:462–480, 2001. doi: 10.1175/1520-0469(2001)058<0462:IBESWA>2.0.CO;2.
- G. J. Boer. A hybrid moisture variable suitable for spectral gcm, research activities in atmospheric and oceanic modelling. *World Meteorological Organization, Geneva*, 21, 1995.
- J. P. Boris and D. L. Book. Flux-corrected transport i: Shasta, a fluid transport algorithm that works. *J. Comp. Phys.*, 11:38–69, 1973.
- W. D. Collins, P. J. Rasch, B. A. Boville, J. J. Hack, J. R. McCaa, D. L. Williamson, J. T. Kiehl, B. Briegleb, C. Bitz, S. Lin, M. Zhang, and Y. Dai. Description of the near community atmosphere model (cam 3.0). *National Center For Atmospheric Research Boulder, Colorado*, 2004.
- D. A. Durrant. *Numerical Methods for Fluid Dynamics With Applications to Geophysics*. Springer-Verlag, 2 edition, 2010.
- A. Engel, T. Möbius, H. Bönisch, U. Schmidt, R. Heinz, I. Levin, E. Atlas, S. Aoki, T. Nakazawa, S. Sugawara, F. Moore, D. Hurst, J. Elkins, S. Schauffler, A. Andrews, and K. Boering. Age of stratospheric air unchanged within uncertainties over the past 30 years. *Nature Geoscience*, 2:28 – 31, 2009. doi: 10.1038/ngeo388.

Bibliography

- P. Jöckel. On a fundamental problem in implementing flux-form advection schemes for tracer transport in 3-dimensional general circulation and chemistry transport models. *Q. J. R. Meteorol. Soc.*, 127:1035–1052, 2001.
- H. Körnich, G. Schmitz, and E. Becker. Dependence of the annular mode in the troposphere and stratosphere on orography and land-sea heating contrasts. *Geophys. Res. Lett.*, 30:1265, 2003. doi: 10.1029/2002GL016327.
- R. J. LeVeque. High resolution conservative algorithms for advection in incompressible flow. *SIAM J. Numer. Anal.*, 33:627–665, 1996.
- T. Minoshima, Y. Matsumoto, and T. Amano. Multi-moment advection scheme for vlasov simulations. *J. Comput. Phys.*, 230:6800–6823, 2011. doi: 10.1016/j.jcp.2011.05.010.
- S. Moorthi, R. W. Higgins, and J. R. Bates. A global multilevel atmospheric model using a vector semi-lagrangian finite-difference scheme. part ii: Version with physics. *Mon. Wea. Rev.*, 123:1523–1541, 1995. doi: 10.1175/1520-0493(1995)123<1523:AGMAMU>2.0.CO;2.
- R. D. Nair and P. H. Lauritzen. A class of deformational flow test cases for linear transport problems on the sphere. *J. Comput. Phys.*, 229:8868–8887, 2010. doi: 10.1016/j.jcp.2010.08.014.
- W. Nolting. *Grundkurs Theoretische Physik 4, Spezielle Relativitätstheorie, Thermodynamik*. Springer-Verlag, 6 edition, 2005.
- O. Pauluis and I. M. Held. Entropy budget of an atmosphere in radiative-convective equilibrium. part i: Maximum work and frictional dissipation. *J. Atmos. Sci.*, 59:125–139, 2002. doi: 10.1175/1520-0469(2002)059<0125:EBOAAI>2.0.CO;2.
- M. J. Prather. Numerical advection by conservation of second-order moments. *J. Geophys. Res.*, 91:6671–6681, 1986. doi: 10.1029/JD091iD06p06671.
- D. Randall. *An Introduction to Atmospheric Modeling*. Department of Atmospheric Science Colorado State University, 1 edition, 2004.

- E. Roeckner, R. Brokopf, M. Esch, M. Giorgetta, S. Hagemann, L. Kornbluh, E. Manzini, U. Schlese, and U. Schulzweida. Sensitivity of simulated climate to horizontal and vertical resolution in the echam5 atmosphere model. *American Meteorological Society, Journal of Climate*, 19, 2006.
- R. B. Rood. Numerical advection algorithms and their role in atmospheric transport and chemistry models. *Rev. Geophys.*, 25:71–100, 1987. doi: 10.1029/RG025i001p00071.
- G. A. Schmidt and Coauthors. Present-day atmospheric simulations using giss models: Comparison to in situ, satellite, and reanalysis data. *American Meteorological Society, Journal of Climate*, 19, 2006.
- J. F. Scinocca, N. A. McFarlane, M. Lazare, J. Li, and D. Plummer. Technical note: The ccm3 third generation agcm and its extension into the middle atmosphere. *Atmos. Chem. Phys.*, 8:7055–7074, 2008. doi: 0.5194/acp-8-7055-2008.
- C. E. Shannon. A mathematical theory of communication. *Bell Syst. Techn. J.*, 27: 379–423, 1948.
- T. G. Shepherd. Transport in the middle atmosphere. *Journal of the Meteorological Society of Japan*, 85:165–191, 2007.
- A. J. Simmons and D. M. Burridge. An energy and angular momentum conserving vertical finite-difference scheme and hybrid vertical coordinates. *Mon. Wea. Rev.*, 109:758–766, 1981.
- G. Thiele and J. L. Sarmiento. Tracer dating and ocean ventilation. *J. Geophys. Res.*, 95:9377–9391, 1990. doi: 10.1029/JC095iC06p09377.
- D. L. Williamson and P. J. Rasch. Water vapor transport in the near ccm2. *Tellus A*, 46:34–51, 1994. doi: 10.1034/j.1600-0870.1994.00004.x.

Acknowledgment

I would like to thank my supervisor, Erich Becker, who supported and guided me with great effort. He inspired and challenged me to develop a deeper understanding of atmospheric science. I am grateful for advices from Heiner Körnich who was a critical mentor and a patient friend. A special thanks to the colleagues and administrative staff of the IAP and MISU for the kind welcome and the great academical and technical support. I thank Lennart Schüler and Benjamin Wolf for their friendship and stimulating discussions. Moreover, I would like to thank my girlfriend, Christin, for her patience and support at all times. Lastly, I offer my regards to all of those who helped me in any respect during the completion of my thesis.

Erklärung

Hiermit versichere ich, dass ich die vorliegende Arbeit selbstständig verfasst und keine außer den angegebenen Hilfsmitteln und Quellen verwendet habe.

Rostock, den 7.2.2012

Mark Schlutow